DEEPLY-VIRTUAL AND PHOTOPRODUCTION OF MESONS AT HIGHER-ORDER AND HIGHER-TWIST*

K. Passek-K.

Division of Theoretical Physics, Ruđer Bošković Institute
Zagreb, Croatia

Both deeply-virtual and photoproduction of mesons offer promising access to generalized parton distributions and complementary description of different kinematical regions. The higher-order contributions offer stabilizing effect with respect to the dependence on renormalization scales, while higher-twist effects have been identified as especially important in the case of the production of pseudo-scalar mesons. This was confirmed by the recent evaluation of the complete twist-3 contribution to π and η/η' photoproduction and its confrontation with experimental data.

1. Introduction

Historically, most of the information about the high-energy nucleon structure came from the deeply inelastic scattering (DIS). From DIS data, one extracts the parton distribution functions (PDFs) being the probabilities that a certain parton is found in a nucleon with a certain longitudinal momentum fraction of the nucleon momentum. Through PDFs, the one-dimensional structure of the nucleon is thus revealed. The hard-exclusive processes offer insight into the transverse distribution of partons and corresponding generalized parton distributions (GPDs) give access to nucleon 3D structure. GPDs are functions of three variables: x, the parton's "average" longitudinal momentum fraction, ξ, the longitudinal momentum transfer (skewness parameter), and t, momentum transfer squared, while their evolution with energy is encapsulated in the dependence on the factorization scale. At leading twist-2, there are eight quark GPDs and eight gluon GPDs classified according to different quantum numbers (parity, chirality), as well as different GPDs for different quark flavours. To reveal their form is thus not an easy task and information from several processes has to be combined.

---

* Presented at the 29th Cracow Epiphany Conference on *Physics at the Electron–Ion Collider and Future Facilities*, Cracow, Poland, 16–19 January, 2023.

For the description of the hard exclusive processes, one employs the handbag mechanism in which only one quark from the incoming nucleon and one from the outgoing nucleon participate in the hard subprocess while all other partons are spectators. The simplest and well-investigated process to which this approach has been applied is the Compton scattering $\gamma^{(*)}N \to \gamma N$, while meson electroproduction $\gamma^{(*)}N \to MN'$ represents the natural extension and offers access to quark flavours. A prerequisite for the handbag mechanism is the presence of at least one large scale, which allows for the use of perturbative expansion in the strong coupling constant and the power, *i.e.*, twist, expansion. Two kinematic regions have been extensively studied: the deeply virtual (DV) region, where the virtuality Q^2 of the incoming photon is large and the momentum transfer $(-t)$ from the incoming to the outgoing nucleon is small; and the wide-angle (WA) region, where $(-t)$, $(-u)$, and s are all large, while Q^2 is smaller than $(-t)$ ($Q^2 = 0$ in the case of photoproduction). Factorization proofs exist for all orders for DV Compton scattering (DVCS) [1] and DV meson production (DVMP) [2], with the process amplitudes factorizing into hard perturbatively calculable subprocess amplitudes and GPDs that encapsulate the soft hadron–parton transitions and the hadron structure. However, general factorization proofs are still lacking for WA processes, although it has been shown that factorization holds to next-to-leading order in the strong coupling for the WA Compton scattering (WACS) [3, 4] and to leading order for the WA meson production (WAMP) [5]. It is argued that in the symmetric frame where skewness is zero, the amplitudes can be represented as a product of subprocess amplitudes and form factors that represent $1/x$ moments of GPDs at zero-skewness.

Both DVCS and WACS were widely investigated in the last decades and the handbag factorization achieved a good description of the experimental data. The leading twist-2 description of DV vector meson production only considers the contributions of longitudinally-polarized photons, specifically $\gamma_{\rm L}^*N \to V_{\rm L}N'$. This description has been observed to be in relatively good agreement with the current experimental data (see [6, 7] and the references therein). However, there is still a lack of systematic separation between longitudinal and transverse experimental data. The contributions of transversely polarized photons $\gamma_{\rm T}^{(*)}N \to V_{\rm L,T}N'$ have also been investigated by including the twist-3 corrections to the meson state [8, 9]. On the other hand, the experimental data for DV pion production [10–13] suggest the high significance of transversely polarized photons, which are not accounted for by the leading twist-2 $\gamma_{\rm L}^*N \to \pi N'$ contributions. As in the vector meson case, a twist-3 calculation has been proposed, which incorporates twist-2 chiral-odd, *i.e.*, transversity (parton helicity flip), GPDs, and twist-3 pion corrections. The calculation including only the twist-3 2-body pion

Fock component (Wandzura–Wilczek approximation) has already achieved a successful agreement with the data [14]. Experimental data for the WA pion production [15–17] also indicate that the twist-2 contributions [5] are not sufficient. But unlike DVMP, the twist-3 contribution to pion photoproduction was found to vanish in the commonly used Wandzura–Wilczek approximation. In [19], both 2- and 3-body twist-3 Fock components of π_0 were considered and successfully fitted to CLAS data [17]. This work was extended to the photoproduction of η and η' mesons [20] and WA electroproduction of $\pi^\pm, \pi^0$ [21]. The application of the latter analytical results for the subprocess amplitudes to the DVMP subprocess amplitudes is straightforward, and the phenomenological analysis is underway.

The DV and WA regions enable complementary access to GPDs at small and large $(-t)$, respectively. A vast amount of experimental data needs to be confronted with reliable theoretical predictions, which should include higher-order perturbative predictions as well as higher-twist contributions. Here, we provide a brief overview of some recent developments.

2. Deeply-virtual meson production at twist-2 and NLO

The DVMP amplitude $\gamma^* N \to M N'$ can be expressed through, so-called, transition form factors

$$^a\mathcal{T}\left(\xi, t, Q^2\right) = \int\limits_{-1}^{1} \frac{\mathrm{d}x}{2\xi} \int\limits_{0}^{1} \mathrm{d}u \, T^a(x, \xi, u, \mu) \, F^a(x, \xi, t, \mu) \, \phi(u, \mu) \qquad (1)$$

with a denoting quark and gluon contributions, and u the longitudinal momentum fraction of the meson's parton. The factorization scale μ separates the short-distance dynamics, represented by the subprocess amplitudes T^a, from the long-distance dynamics represented by the hadron wave functions: the GPD F^a and the meson distribution amplitude (DA) ϕ.

Transition form factors $^a\mathcal{T}$ have a similar role in DVMP as Compton form factors in DVCS, but they additionally depend on meson DA, *i.e.*, meson structure, making the analysis of the process both more challenging, as well as, potentially more rewarding. In contrast to DVCS, DVMP enables easy access to GPDs of different quark flavours and offers the natural distinction of GPDs of different parity: at twist-2 chiral-even GPDs, H^q, E^q contribute to the production of longitudinally polarized vector mesons (V_L) and scalar (S) mesons, while $\widetilde{H}^q$ and $\widetilde{E}^q$ appear in the production of pseudoscalar (P) and axial-vector (A_L) mesons. Moreover, the contribution of gluon GPDs H^g, E^g $(\widetilde{H}^g, \widetilde{E}^g)$ to the production of neutral V_L (A_L) mesons is more significant since, unlike in DVCS, they contribute already at the leading order. Therefore, their form is phenomenologically more accessible.

The twist-2 DVMP subprocess amplitudes $\gamma_{\mathrm{L}}^* q \to (q\bar{q})q$ and $\gamma_{\mathrm{L}}^* g \to (q\bar{q})g$ are calculated perturbatively order by order in the strong coupling constant

$$T^a(x,\xi,u,\mu) = \frac{\alpha_{\mathrm{s}}(\mu_{\mathrm{R}})}{4\pi}T^{a(1)}(x,\xi,u) + \frac{\alpha_{\mathrm{s}}^2(\mu_{\mathrm{R}})}{(4\pi)^2}T^{a(2)}(x,\xi,u,\mu_{\mathrm{R}},\mu) + \cdots \quad (2)$$

and they have been determined to next-to-leading order (NLO) for flavour non-singlet and singlet P and V_{L} mesons [22–24], as well as for the (crossed) production of S and A_{L} mesons [24, 25]. Predictions at finite order are inherently dependent on the renormalization scale μ_{R} and scheme, introducing additional theoretical uncertainty. Therefore, the inclusion of higher-order corrections is crucial to reduce this dependence and stabilize predictions. Although meson DAs (ϕ) and GPDs (F^a) are intrinsically nonperturbative quantities, their evolution can be calculated perturbatively. The complete closed form is known to the NLO order [26], and more recently, NNLO contributions to the evolution kernels have been obtained [27].

The evolution is simpler to implement in the conformal momentum representation. Conformal moments are analogous to the Mellin moments in DIS and represent the moments with respect to the eigenfunctions of the leading order evolution kernels, *i.e.*, with respect to the Gegenbauer polynomials $C_n^{3/2}$ and $C_n^{5/2}$ for quarks and gluon, respectively. The convolution over x and u in transition form factors (1) is thus replaced by the summation over conformal moments, and consequently, the series is summed using the Mellin–Barnes integral over complex conformal moment j [25]

$$^a\mathcal{T}\left(\xi,t,Q^2\right) = \frac{1}{2i}\int\limits_{c-i\infty}^{c+i\infty} \mathrm{d}j\left[i \pm \left\{\begin{matrix}\tan\\\cot\end{matrix}\right\}\left(\frac{\pi j}{2}\right)\right]\xi^{-j-1}$$
$$\times \left[T_{jk}^a(\mu) \overset{k}{\otimes} \phi_k(\mu)\right]F_j^a(\xi,t,\mu). \quad (3)$$

This approach has been developed and extensively applied to DVCS [28], and then extended to DVMP. Regardless of whether one considers the Compton or transition form factors in momentum fraction (1) or conformal momentum space (3), a complete deconvolution is impossible, and GPD access is only possible through different modelling approaches. Dedicated software is now available: PARTONS [29] and Gepard [30] for analysis in momentum fraction and conformal momentum space, respectively. The DVV_{L}P is included in the latter.

While there has been a lot of interest in the DVCS process, there are relatively few NLO phenomenological analyses of the DVMP process [22, 25, 31], despite the availability of experimental data. The complete set of x and j space analytical results for all meson channels can be found in [24, 25]. The numerical analysis performed there shows that NLO corrections are important and model-dependent (Fig. 1). The effects of LO GPD and DA evolution are significant and for NLO calculations, one should include also NLO evolution. Gluon corrections play a significant role in small ξ production of vector mesons, and there may be a need for resummation of the large logarithmic $\ln(1/\xi)$ terms observed in both gluon evolution and gluon coefficient function. Finally, the choice of meson distribution amplitude is found to have a significant impact on the results.
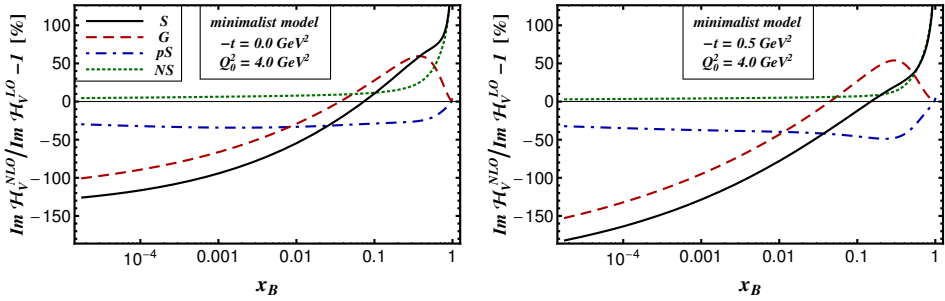

Fig. 1. Relative NLO corrections to the imaginary part of the flavor singlet TFF (solid) broken down to the gluon (dashed), pure singlet quark (dash-dotted), and 'non-singlet' quark (dotted) contributions (Ref. [25]).

Since GPDs are process-independent quantities, the simultaneous description and global fits of GPDs to DIS, DVCS, and DVMP data represent the next necessary step. Through these, one hopes to gain additional information on the importance and stability of NLO predictions and the validity of different models. Using the conformal momentum representation [25], the first global fits on DIS, DVCS, and DVV_LP small-x HERA collider data have been performed at LO [32] ($\chi^2/n_\mathrm{dof} \approx 2$), and at NLO [33] (Bayesian analysis). The recent NLO analysis using corrected NLO analytical results [24] and Gepard software shows promising agreement of theory and experiment ($\chi^2/n_\mathrm{dof} = 254.3/231$) and indicates that a global description of DVCS and DVV_LP is reachable at NLO (Fig. 2).
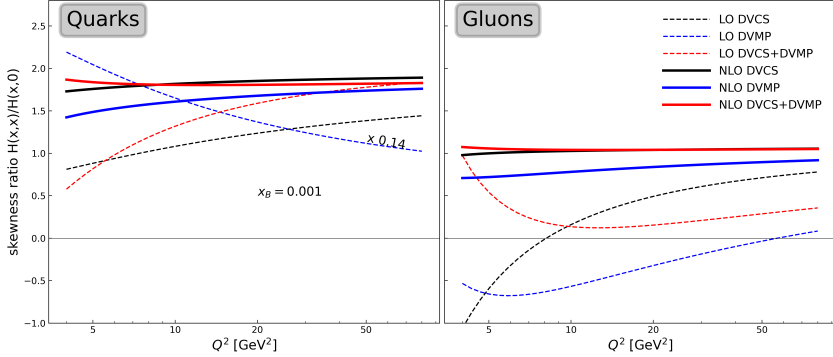
Fig. 2. Skewness ratio for GPD H (preliminary K. Kumerički, Transversity 2022).

3. Pseudoscalar meson production at higher-twist

The twist-3 LO prediction for the electroproduction of the pseudoscalar meson P, which includes 2- and 3-body meson Fock states, was first calculated for the WA region [21]. Here, we review the findings and their confrontation with experimental data for photoproduction ($Q^2 = 0$). The analytical expressions obtained for the subprocess amplitudes can also be applied to the DVPP analysis ($t \to 0$).

The helicity amplitudes for $\gamma^{(*)}N \to PN'$ process in the WA angle region can be expressed in terms of the subprocess amplitudes $\mathcal{H}$ multiplied by the soft form factors, R_i^P and S_i^P, which represent $1/x$-moments of zero-skewness GPDs $\int_0^1 \frac{\mathrm{d}x}{x} F_i^a(x,t)$. The R-type form factors are related to the helicity non-flip GPDs H, $\widetilde{H}$, and E. The S-type form factors are related to the helicity-flip or transversity GPDs H_{T}, $\bar{E}_{\mathrm{T}}$, and $\widetilde{H}_{\mathrm{T}}$[1].

The amplitudes $\mathcal{H}$ correspond to the subprocesses $\gamma^{(*)}q \to Pq'$ and they are calculated using handbag diagrams as the ones depicted in Fig. 3. The meson P is replaced by an appropriate 2- or 3-body Fock state. The projector $\pi \to q\bar{q}$ contributes to the subprocess amplitudes corresponding to the diagrams depicted in Fig. 3 (a) and its structure is given by

$$\mathcal{P}_2^P \sim f_\pi \left\{ \gamma_5 \not{p}\, \phi_\pi(u,\mu) + \mu_\pi(\mu)\gamma_5 \Big[\phi_{\pi p}(u,\mu) - [\ldots]\phi'_{\pi\sigma}(u,\mu) + [\ldots]\phi_{\pi\sigma}(u,\mu) \Big] \right\}. \tag{4}$$

The first term in (4) corresponds to the twist-2 part, while the twist-3 part is proportional to the chiral condensate $\mu_\pi = m_\pi^2/(m_u + m_d) \cong 2$ GeV (at the factorization scale $\mu_{\mathrm{F}} = 2$ GeV). This parameter is large and although the twist-3 cross section for pion electroproduction is suppressed by μ_π^2/Q^2

---

[1] The GPDs $\tilde{E}$ and $\tilde{E}_{\mathrm{T}}$ and their associated form factors decouple at zero skewness.

as compared to the twist-2 cross section, for the range of Q^2 accessible in current experiments, the suppression factor is of the order of unity[2]. The 3-body $\pi \to q\bar{q}g$ projector contributes to the amplitudes corresponding to Fig. 3 (b)

$$\mathcal{P}_3^P \sim f_{3\pi}(\mu)\gamma_5[\ldots]\,\phi_{3\pi}(u_1, u_2, u_g, \mu)\,. \tag{5}$$

The helicity non-flip amplitudes are generated by twist-2, while the helicity flip ones are of twist-3 origin.
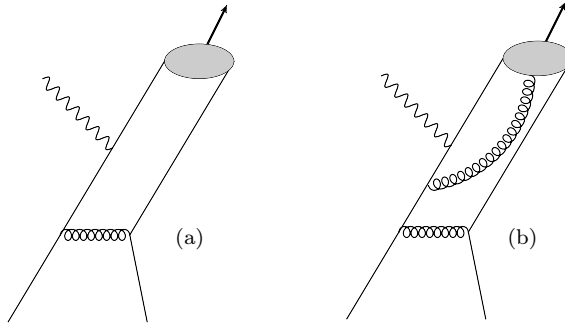

Fig. 3. Generic diagrams for 2- and 3-body subprocess amplitudes.

In addition to twist-2 DA ϕ_π, there are two 2-body twist-3 DAs, $\phi_{\pi p}$ and $\phi_{\pi\sigma}$, and 3-body twist-3 DA $\phi_{3\pi}$. Twist-3 DAs are connected by equations of motion (EOMs). By EOMs and DA symmetry properties, it is possible to express the twist-3 subprocess amplitudes in terms of only two twist-3 DAs, and combine 2- and 3-body contributions. Applying EOMs also results in an inhomogeneous linear first-order differential equation, which can be used to determine $\phi_{\pi p}$ (and $\phi_{\pi\sigma}$) from a known 3-body DA $\phi_{3\pi}$ [34][3] .

In meson electroproduction, both transverse and longitudinal photons contribute to twist-2 subprocess amplitudes. As expected, the longitudinal contribution vanishes in the photoproduction limit, while in the DVMP limit, only longitudinal photons contribute. The general structure of the twist-3 contributions for both transverse and longitudinal photons reads

$$\begin{aligned}
\mathcal{H}^{P,\mathrm{tw3}} &= \mathcal{H}^{P,\mathrm{tw3},q\bar{q}} + \mathcal{H}^{P,\mathrm{tw3},q\bar{q}g} \\
&= \left(\mathcal{H}^{P,\phi_{\pi p}} + \underbrace{\mathcal{H}^{P,\phi_{\pi 2}^{\mathrm{EOM}}}}_{} \right) + \left(\underbrace{\mathcal{H}^{P,q\bar{q}g,C_\mathrm{F}}}_{} + \mathcal{H}^{P,q\bar{q}g,C_\mathrm{G}} \right) \\
&= \mathcal{H}^{P,\phi_{\pi p}} + \mathcal{H}^{P,\phi_{3\pi},C_\mathrm{F}} + \mathcal{H}^{P,\phi_{3\pi},C_\mathrm{G}}\,, \tag{6}
\end{aligned}$$

---

[2] Twist-3 effects can also be generated by twist-3 GPDs. However, these are expected to be small and therefore neglected.

[3] It is important to note that the same gauge must be used consistently for the constituent gluon in the $q\bar{q}g$ projector and EOMs.

where $\mathcal{H}^{P,\text{tw3},q\bar{q}}$ is the twist-3 2-body contribution proportional to the C_{F} color factor, and $\mathcal{H}^{P,\text{tw3},q\bar{q}g}$ is the twist-3 3-body contribution with C_{F} and C_{G} proportional parts. The C_{G} part is gauge invariant, whereas for C_{F} contributions, only the sum of 2- and 3-body parts is gauge invariant with respect to the choice of photon or virtual gluon gauge. EOMs are used to obtain this sum, as well as the complete twist-3 contribution expressed through only two twist-3 DAs, $\phi_{3\pi}$ and $\phi_{\pi p}$. The twist-3 subprocess amplitude for longitudinal photons vanishes both for photoproduction and DVMP. One finds that for photoproduction $\mathcal{H}^{P,\phi_{\pi p}} = 0$ [19]. For DVMP, $\mathcal{H}^{P,\phi_{\pi 2}^{\text{EOM}}} = 0$, and while no end-point singularities are present for $t \neq 0$, they must be considered in the limit $t \to 0$ since for $\mathcal{H}^{P,\phi_{\pi p}} \sim \int_0^1 \frac{du}{u} \phi_{Pp}(u)$. In [14], the modified hard-scattering picture has been used to regularize the 2-body contributions. With the complete twist-3 contribution now available [21], the analysis in modified and a collinear picture is underway.

In [19], the cross section for π^0 photoproduction has been fitted to [17] data. The results are displayed in Fig. 4. The twist-2 prediction lies well below the data. However, by including the twist-3 contributions, one obtains reasonable agreement with the experiment. Twist-3 is more important in the backward hemisphere (θ is c.m.s. scattering angle). In [21], the analysis was extended to π^+ and π^-, using only a few available experimental data [15, 16]. In [20], η (preliminary GlueX data) and η' photoproduction was studied. A similar behavior in photoproduction cross sections was observed, except for η', where the twist-2 contribution was significant, offering the possibility of determining the 2-gluon twist-2 DA.
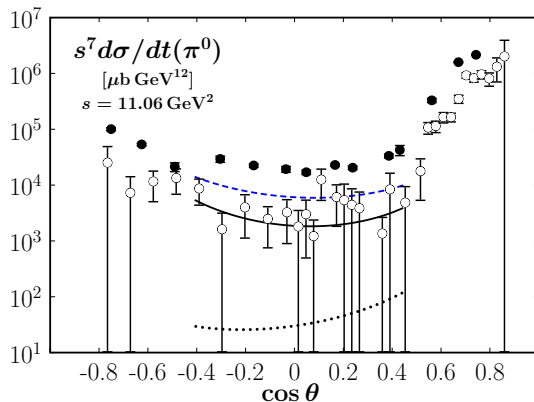

Fig. 4. The cross section for π^0 photoproduction with twist-3 contributions. Solid (dotted) curve: full (twist-2) result. Dashed curve: full result with fixed renormalization and factorization scale. Data taken from CLAS [17] (open circles) and from SLAC [15] ($s = 10.3$ GeV^2) (Ref. [21]).

For pion electroproduction, there are four partial cross sections. In [21], the theoretical predictions were given and the importance of the measurement was stressed. Different combinations of form factors make it possible to extract transversity GPDs (F_T^q), which have a large ($-t$) behavior that is important for parton tomography.

In meson photoproduction, spin-dependent observables such as the correlations of the helicities of the photon and either the incoming or outgoing nucleon, *i.e.*, A_{LL} and K_{LL}, offer additional insight that is less sensitive to particular parameters. It can be shown that $A_{LL}^{P,\mathrm{tw2}} = K_{LL}^{P,\mathrm{tw2}}$ and $A_{LL}^{P,\mathrm{tw3}} = -K_{LL}^{P,\mathrm{tw3}}$, indicating that the measurement of A_{LL} and K_{LL} offers a characteristic signature for the dominance of twist-2 or twist-3, similar to the role that the comparison of σ_T and σ_L has in DVMP. From Fig. 5, it is clear that our numerical results suggest the dominance of twist-3 for large θ, while twist-2 increases in the forward direction.
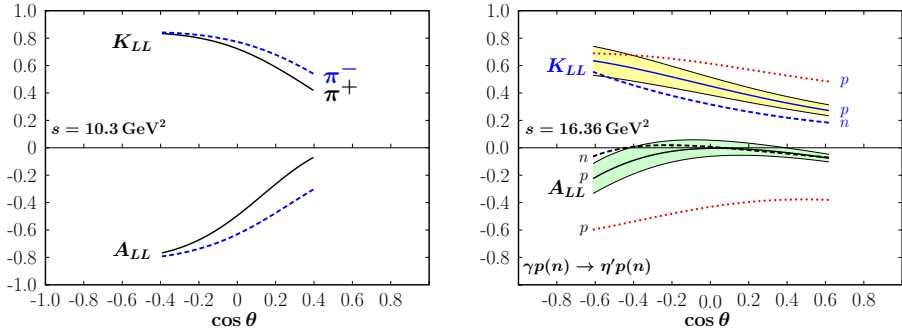

Fig. 5. Results for the helicity correlation parameters A_{LL} and K_{LL} for π^+, π^-, and η' photoproduction (Refs. [20, 21]).

4. Summary and outlook

Twist-2 NLO contributions to DVMP amplitudes are available and need to be compared with experimental data. The preliminary comparison of vector meson production to data seems satisfactory, but NLO corrections are significant, and the first DIS, DVCS, and DVV_LP fits have been performed. For pseudoscalar meson production, twist-3 contributions dominate, and a complete analysis of 2- and 3-body twist-3 contributions is ongoing. The available twist-2 NLO contributions should also be tested. It is important to note that the choice of meson distribution amplitude significantly affects the DVMP predictions. In WA photoproduction of π mesons, the twist-2 analysis falls short by an order of magnitude. The complete twist-3 contribution has been included, and it was found that the meson's twist-3 contributions dominate for πs and η. Future experimental goals include the clear separation of longitudinally- and transversely-polarized photon contributions.

REFERENCES

[1] J.C. Collins, A. Freund, *Phys. Rev. D* **59**, 074009 (1999), `arXiv:hep-ph/9801262`.

[2] J.C. Collins, L. Frankfurt, M. Strikman, *Phys. Rev. D* **56**, 2982 (1997), `arXiv:hep-ph/9611433`.

[3] A.V. Radyushkin, *Phys. Rev. D* **58**, 114008 (1998), `arXiv:hep-ph/9803316`.

[4] M. Diehl, T. Feldmann, R. Jakob, P. Kroll, *Eur. Phys. J. C* **8**, 409 (1999), `arXiv:hep-ph/9811253`.

[5] H.W. Huang, P. Kroll, *Eur. Phys. J.* **C17**, 423 (2000), `arXiv:hep-ph/0005318`.

[6] H1 Collaboration (F.D. Aaron *et al.*), *J. High Energy Phys.* **2010**, 032 (2010), `arXiv:0910.5831 [hep-ex]`.

[7] COMPASS Collaboration (C. Adolph *et al.*), *Nucl. Phys. B* **865**, 1 (2012), `arXiv:1207.4301 [hep-ex]`.

[8] I.V. Anikin, O.V. Teryaev, *Phys. Lett. B* **554**, 51 (2003), `arXiv:hep-ph/0211028`.

[9] S.V. Goloskokov, P. Kroll, *Eur. Phys. J. C* **74**, 2725 (2014), `arXiv:1310.1472 [hep-ph]`.

[10] HERMES Collaboration (A. Airapetian *et al.*), *Phys. Lett. B* **682**, 345 (2010), `arXiv:0907.2596 [hep-ex]`.

[11] CLAS Collaboration (I. Bedlinskiy *et al.*), *Phys. Rev. Lett.* **109**, 112001 (2012), `arXiv:1206.6355 [hep-ex]`.

[12] JLab Hall A Collaboration (M. Defurne *et al.*), *Phys. Rev. Lett.* **117**, 262001 (2016), `arXiv:1608.01003 [hep-ex]`.

[13] JLab Hall A Collaboration (M. Dlamini *et al.*), *Phys. Rev. Lett.* **127**, 152301 (2021), `arXiv:2011.11125 [hep-ex]`.

[14] S.V. Goloskokov, P. Kroll, *Eur. Phys. J. C* **65**, 137 (2010), `arXiv:0906.0460 [hep-ph]`.

[15] R.L. Anderson *et al.*, *Phys. Rev. D* **14**, 679 (1976).

[16] JLab Hall A, JLab E94-104 Collaboration (L.Y. Zhu *et al.*), *Phys. Rev. C* **71**, 044603 (2005), `arXiv:nucl-ex/0409018`.

[17] CLAS Collaboration (M.C. Kunkel *et al.*), *Phys. Rev. C* **98**, 015207 (2018), `arXiv:1712.10314 [hep-ex]`.

[18] H.W. Huang, R. Jakob, P. Kroll, K. Passek-Kumerički, *Eur. Phys. J. C* **33**, 91 (2004), `arXiv:hep-ph/0309071`.

[19] P. Kroll, K. Passek-Kumerički, *Phys. Rev. D* **97**, 074023 (2018), `arXiv:1802.06597 [hep-ph]`.

[20] P. Kroll, K. Passek-Kumerički, *Phys. Rev. D* **105**, 034005 (2022), `arXiv:2111.08965 [hep-ph]`.

[21] P. Kroll, K. Passek-Kumerički, *Phys. Rev. D* **104**, 054040 (2021), `arXiv:2107.04544 [hep-ph]`.

[22] A.V. Belitsky, D. Müller, *Phys. Lett. B* **513**, 349 (2001), `arXiv:hep-ph/0105046`/.

[23] D.Y. Ivanov, L. Szymanowski, G. Krasnikov, *JETP Lett.* **80**, 226 (2004), `arXiv:hep-ph/0407207`.

[24] G. Duplančić, D. Müller, K. Passek-Kumerički, *Phys. Lett. B* **771**, 603 (2017), `arXiv:1612.01937 [hep-ph]`.

[25] D. Müller, T. Lautenschlager, K. Passek-Kumerički, A. Schäfer, *Nucl. Phys. B* **884**, 438 (2014), `arXiv:1310.5394 [hep-ph]`.

[26] A.V. Belitsky, D. Müller, L. Niedermeier, A. Schäfer, *Nucl. Phys. B* **546**, 279 (1999), `arXiv:hep-ph/9810275`.

[27] V.M. Braun, A.N. Manashov, S. Moch, M. Strohmaier, *J. High Energy Phys.* **2017**, 037 (2017), `arXiv:1703.09532 [hep-ph]`.

[28] K. Kumerički, D. Müller, K. Passek-Kumerički, *Nucl. Phys. B* **794**, 244 (2008), `arXiv:hep-ph/0703179`.

[29] B. Berthou *et al.*, *Eur. Phys. J. C* **78**, 478 (2018), `arXiv:1512.06174 [hep-ph]`.

[30] K. Kumerički, `https://github.com/kkumer/gepard`, `https://gepard.phy.hr/`

[31] M. Diehl, W. Kugler, *Eur. Phys. J. C* **52**, 933 (2007), `arXiv:0708.1121 [hep-ph]`.

[32] M. Meskauskas, D. Müller, *Eur. Phys. J. C* **74**, 2719 (2014), `arXiv:1112.2597 [hep-ph]`.

[33] T. Lautenschlager, D. Müller, A. Schäfer, `arXiv:1312.5493 [hep-ph]`.

[34] V.M. Braun, I.E. Filyanov, *Z. Phys. C* **48**, 239 (1990).